Kinematic Effects on Probability Density Functions of Energy Dissipation Rate and Enstrophy in Turbulence

Toshiyuki Gotoh,[1,2,*] Takeshi Watanabe,[1,†] and Izumi Saito[1,‡]
[1]Department of Physical Science and Engineering, Nagoya Institute of Technology, Gokiso, Nagoya 466-8555, Japan
[2]Research and Education Center for Natural Sciences, Keio University, Hiyoshi, Yokohama 223-8521, Japan

(Received 17 November 2022; revised 27 March 2023; accepted 30 May 2023; published 22 June 2023)

Direct numerical simulation and theoretical analyses showed that the probability density functions (PDFs) of the energy dissipation rate and enstrophy in turbulence are asymptotically stretched gamma distributions with the same stretching exponent, and both the left and right tails of the enstrophy PDF are longer than those of the energy dissipation rate regardless of the Reynolds number. The differences in PDF tails arise due to the kinematics, with differences in the number of terms contributing to the dissipation rate and enstrophy. Meanwhile, the stretching exponent is determined by the dynamics and likeliness of singularities.

DOI: 10.1103/PhysRevLett.130.254001

In turbulence, kinetic energy is pumped into the flow at large scales of motion and transferred to smaller scales by nonlinear interactions among fluid motions of various sizes, and then dissipated into heat under the action of the viscosity. In a statistically steady state, the means of the input rate and transfer rate are equal to the mean of the dissipation rate of the kinetic energy per unit mass, which is defined by $\bar{\epsilon} = \langle \tilde{\epsilon}(\boldsymbol{x}, t) \rangle$ and $\tilde{\epsilon}(\boldsymbol{x}, t) = (\nu/2)(\partial u_i/\partial x_j + \partial u_j/\partial x_i)^2$, where $\langle\rangle$ denotes the ensemble average, and summation over repeated indices is assumed. Therefore, the dissipation rate is a key factor connecting large-, intermediate-, and small-scale turbulence dynamics. However, very strong fluctuations of the dissipation rate occur often; the extreme amplitude is beyond thousands of times the mean, and the probability density function (PDF) $P(\epsilon)$ for $\epsilon = \tilde{\epsilon}/\bar{\epsilon}$ expands rightward as the Reynolds number R_λ increases. Vorticity refers to the swirling motion of fluid, while enstrophy (squared vorticity), which is defined by $\tilde{\Omega}(\boldsymbol{x}, t) = \tilde{\boldsymbol{\omega}}^2 = (\partial u_i/\partial x_j - \partial u_j/\partial x_i)^2/2$, characterizes the turbulent flow structure (where domains of large enstrophy are of the form of thin tubes distributed randomly and/or coherently). The enstrophy fluctuations are also comparable to, or even stronger than the dissipation, and the right tail of the PDF $P(\Omega)$ for $\Omega = \tilde{\Omega}/\bar{\Omega}$, where $\bar{\Omega}$ is the mean, also expands with increases in R_λ. These strong fluctuations of the dissipation and enstrophy are now widely recognized as the intermittency of turbulence and remain among the central problems in turbulence research.

Since the 1990s, it has been known that the dissipation PDF decays faster than the enstrophy PDF [1–11]. Indeed, as shown in Fig. 1(a), the right tails of $P(\epsilon)$ and $P(\Omega)$ of homogeneous isotropic turbulence (HIT) obtained by direct numerical simulation (DNS) of the Navier-Stokes (NS) equation for an incompressible fluid become very long with increases in R_λ; the right tail of $P(\Omega)$ is longer than that of $P(\epsilon)$, suggesting that the intermittency of the enstrophy is stronger than that of dissipation.

This is curious, however, because dissipation and enstrophy are computed as squared sums of the symmetric or skew-symmetric combination of the same velocity gradients. There have been a number of efforts, including theoretical analyses [2], experimental studies using particle image velocimetry at $R_\lambda = 54$ [3], and high-resolution DNS of HIT up to $R_\lambda = 1300$ with $12\,288^3$ grid points [4–12], to understand the asymptotic behavior of two PDFs. DNS studies showed that the right tails of the PDFs are asymptotically of the stretched exponential, as

$$P_\alpha(x)dx \propto \exp\left(-B_\alpha x^{\beta_\alpha}\right)dx, \quad \text{for } x \gg 1, \tag{1}$$

where x represents the variables ϵ or Ω, and α denotes the labels ϵ or Ω for parameters or PDFs throughout this Letter. The exponents β_ϵ and β_Ω are close to each other, and the Reynolds number dependency of the decay rate B_α is explored [6,12]. However, no satisfactory explanations have yet been proposed for these phenomena, and our knowledge is very limited.

The question to be addressed herein is, why does the enstrophy PDF have a longer tail than the dissipation PDF? We begin with considering two PDFs for the multivariate Gaussian random and solenoidal velocity field, for which the analytical forms of the PDFs were recently obtained by one of the authors [10]. The theory predicts that in the $d(\geq 2)$ dimensional space the PDFs for the dissipation and enstrophy are given by the gamma distribution as

$$P_G(\epsilon)\mathrm{d}\epsilon = \frac{1}{Z_\epsilon}\epsilon^{\frac{N_\epsilon}{2}-1}\exp\left(-\frac{N_\epsilon}{2}\epsilon\right)\mathrm{d}\epsilon, \tag{2}$$

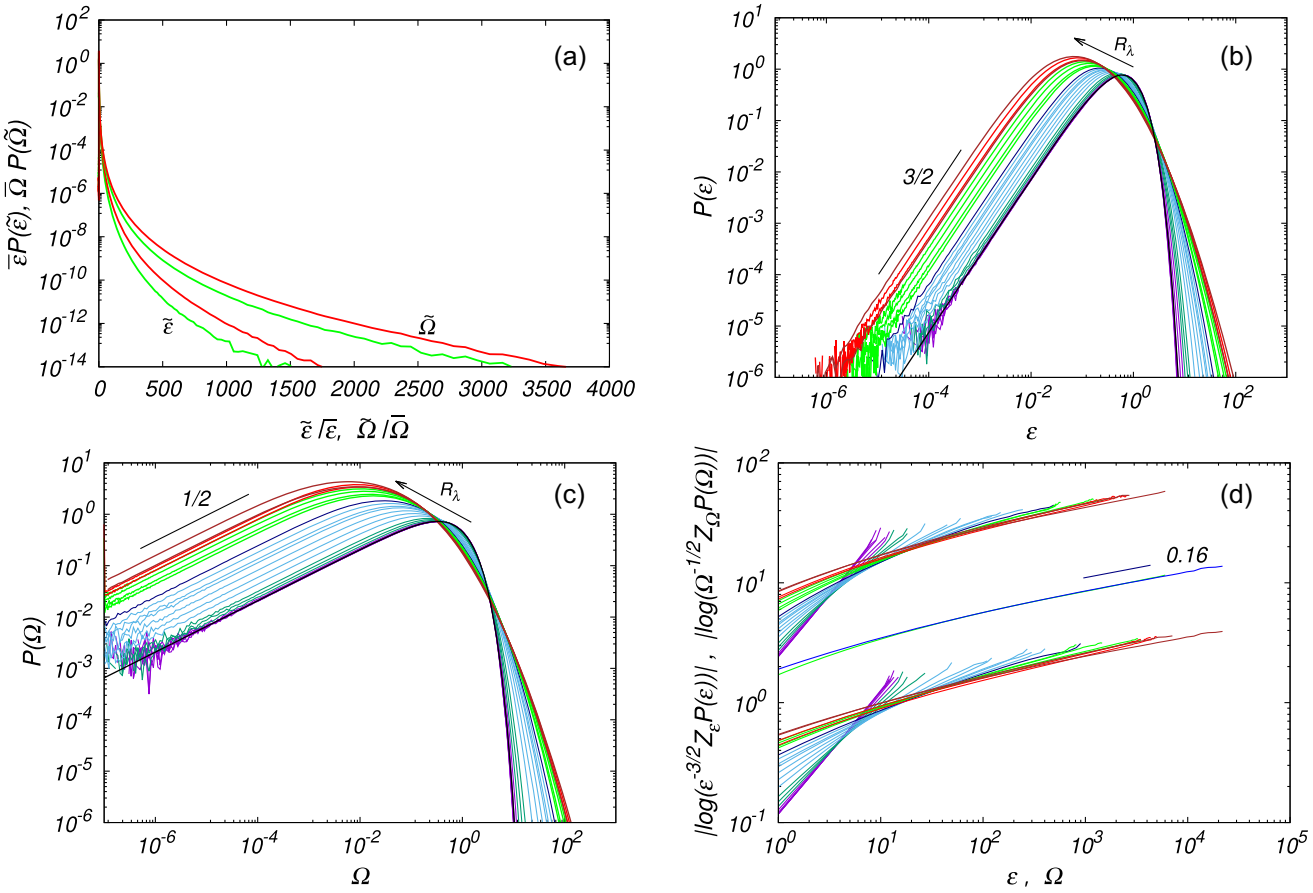

FIG. 1. Probability density functions for the kinetic energy dissipation rate and squared vorticity (enstrophy) of HIT obtained by DNS of NS equation. (a) Upper two curves, $P(\Omega)$. Lower two curves, $P(\epsilon)$. Green, $R_\lambda = 392$; red, $R_\lambda = 1016$. (b) Variation of $P(\epsilon)$ for $\epsilon = \tilde{\epsilon}/\bar{\epsilon}$ against R_λ. (c) $P(\Omega)$ for $\Omega = \tilde{\Omega}/\bar{\Omega}$. Black, gamma distributions Eqs. (2) and (3), respectively. Magenta, $R_\lambda = [0.13, 0.36, 0.61, 1.0, 2.1, 3.8]$; green, $R_\lambda = [6.2, 9.2, 13]$; cyan, $R_\lambda = [23, 32, 44, 58, 66, 84]$; navy, $R_\lambda = 112$; light green, $R_\lambda = [166, 277, 392, 466]$; orange, $R_\lambda = 810$; red, $R_\lambda = 1016$. Brown, $R_\lambda = [650, 1300]$; data due to Buaria *et al.* [8,9,11]. Straight lines show the slopes of 3/2 and 1/2, respectively. (d) Right tails of the compensated PDFs $|\ln[\epsilon^{-3/2}Z_\epsilon P(\epsilon)]|$ (upper curves) and $|\ln[\Omega^{-1/2}Z_\Omega P(\Omega)]|$ (lower curves, shifted by 0.1). The two curves in the middle are the same plots of the dissipation (blue) and enstrophy (green) at $R_\lambda = 1300$ (DNS by Buaria *et al.* [8,9,11]) but are shifted by some amount. The straight line indicates the slope, 0.16.

$$P_G(\Omega)\mathrm{d}\Omega = \frac{1}{Z_\Omega}\Omega^{\frac{N_\Omega}{2}-1}\exp\left(-\frac{N_\Omega}{2}\Omega\right)\mathrm{d}\Omega, \qquad (3)$$

where Z_α is the normalization constant. The N_ϵ and N_Ω are the number of terms contributing to the dissipation and enstrophy for the incompressible fluid, and are functions of d as

$$N_\epsilon = (d+2)(d-1)/2. \qquad N_\Omega = d(d-1)/2, \quad (4)$$

respectively, where the symmetry (skew-symmetry) of the rate of strain (vorticity) tensor and the incompressibility condition are used. Then we have $N_\epsilon = 5$ and $N_\Omega = 3$, respectively, in three-dimensional space [10,12]. It follows from Eqs. (2) and (3) that the N_ϵ (N_Ω) determines the functional form of the left and right tails of $P_G(\epsilon)$ [$P_G(\Omega)$]. When turbulence is excited by the Gaussian random force at low Reynolds number, it is expected that $P(\epsilon)$ and $P(\Omega)$ are close to Eqs. (2) and (3), respectively, and that $B_\epsilon = 5/2$, $B_\Omega = 3/2$, and the exponents are identical as $\beta_\epsilon = \beta_\Omega = 1$. Therefore, for small and large amplitudes, we have

$$P(\epsilon) < P(\Omega) \quad \text{for } R_\lambda < O(1). \qquad (5)$$

To explore the variation of the PDFs with respect to R_λ, we made a set of DNSs of the HIT for $R_\lambda = 0.13$ to 1016 and included the data provided from Buaria and his coworkers [8,9,11]. Details of the simulation and the data are described in the Supplemental Material [10,13,14]. Figures 1(b) and 1(c) show that, when R_λ is very low, the DNS curves follow the gamma distribution (black line). Moreover, even for $R_\lambda = 1300$ the curves of the left tail

remain straight lines with the same slope as that in the Gaussian case, meaning that the left PDF tails obey the power law as $P(\epsilon) \propto \epsilon^{3/2}$ and $P(\Omega) \propto \Omega^{1/2}$, respectively, while the right tails decay more slowly than the exponential and gradually expand rightward with increasing R_λ, suggesting stretched exponential decay. Assuming that for large amplitudes x the PDFs are of the form of

$$P_\alpha(x)dx = \frac{1}{Z_\alpha} x^{N_\alpha/2-1} \exp(-B_\alpha x^{\beta_\alpha})dx, \tag{6}$$

we examined the right PDF tails by fitting the compensated PDFs $|\ln(x^{-N_\alpha/2+1} Z_\alpha P(x))|$ as in Fig. 1(d). The upper group of curves is for ϵ, and the lower group is for Ω. A common feature of the curves is that as R_λ increases, near the right end of the curves, (1) the straight portion of the curve becomes longer, (2) their slopes decrease slowly, and (3) the slopes of the dissipation and enstrophy for a given R_λ are very close to each other, especially when the two curves at $R_\lambda = 1300$ are shifted vertically by some amount, as in the middle of Fig. 1(d); they collapse excellently at large amplitudes [9,11].

The above observations of PDFs confirm that the asymptotic PDF tails at high Reynolds number are stretched exponential [Eq. (6)], and β_ϵ and β_Ω are equal to each other [6,7,9] (for passive scalar dissipation, see Ref. [15]), but the Reynolds number dependency of β_α has not been studied, and the focus has rather been on B_α under the assumption that β_α is independent of R_λ [7]. By analyzing the DNS data, it was found that $B_\alpha = (AR_\lambda^{-\xi})^{\beta_\alpha}$, indicating slower decay of the PDF with R_λ, where A and ξ are positive constants.

We show in Fig. 2(a) the variation of β_ϵ and β_Ω with error bars for low to high Reynolds numbers. It can clearly be seen that β_ϵ and β_Ω are equal within the error bar (see the Supplemental Material [13]).

For very low R_λ, the β_α is slightly larger than unity. This is because the PDFs are those of the Navier-Stokes field excited by the Gaussian random force and not those of the Gaussian random field itself. The excited velocity (gradient) field undergoes strong attenuation by the viscosity, which suppresses the large dissipation rate and enstrophy; therefore, the right PDF tails decay faster than the exponential. They begin to decrease at about $R_\lambda \approx 2$ [10], turn to be a very slow decay for $R_\lambda > 100$, and are slightly smaller than 0.2 for large R_λ, which is well within the range of values reported previously [6,7,9,11]. It is not certain whether β continues to decrease or approaches to a finite positive constant. However, the fact that the two stretching exponents β_ϵ and β_Ω are equal and decrease monotonically with R_λ is sufficient for the arguments presented below.

From the above observations, we tentatively assume that the PDFs of the dissipation rate and enstrophy obey the

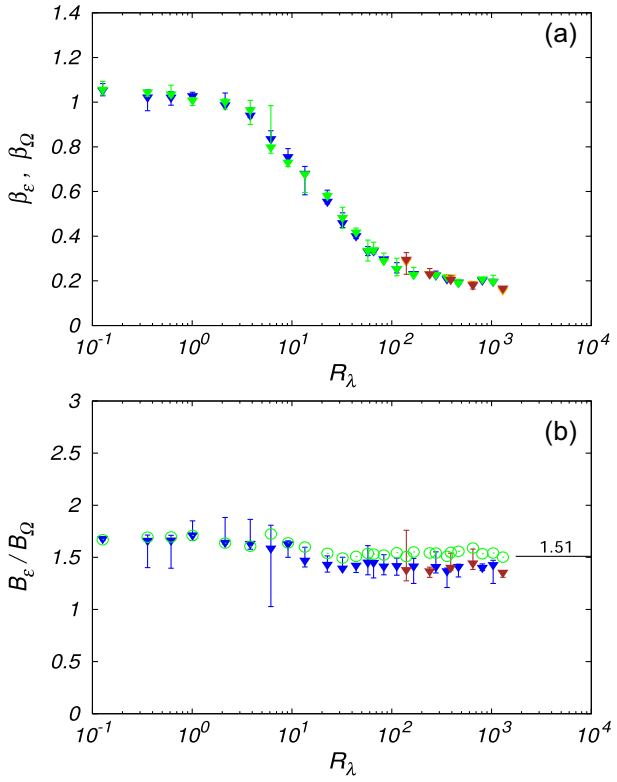

FIG. 2. Variation of (a): β_ϵ (green) and β_Ω (blue). (b): B_ϵ/B_Ω against R_λ obtained by DNS. Filled triangles with error bars, DNS; open circles, theory [Eq. (10)] with use of β of DNS. The error bars were computed by shifting the fitting range by $\pm 50\%$. Symbols of brown for ϵ and orange for Ω are data due to DNSs in Refs. [8,9,11].

stretched gamma distributions with *the same stretching exponent* β for all x:

$$P_\alpha(x)dx = \frac{1}{Z_\alpha} x^{N_\alpha/2-1} \exp\left[-(b_\alpha x)^\beta\right]dx, \tag{7}$$

where $B_\alpha = b_\alpha^\beta$. When the normalization condition and mean of unity are imposed,

$$\int_0^\infty P_\alpha(x)dx = 1, \qquad \int_0^\infty x P_\alpha(x)dx = 1, \tag{8}$$

the constants Z_α and b_α are expressed in terms of the single parameter, β. The results are

$$\frac{1}{Z_\alpha} = \frac{\beta b_\alpha^{N_\alpha/2}}{\Gamma\left(\frac{N_\alpha}{2\beta}\right)}, \qquad b_\alpha = \frac{\Gamma\left(\frac{N_\alpha+2}{2\beta}\right)}{\Gamma\left(\frac{N_\alpha}{2\beta}\right)}, \tag{9}$$

where $\Gamma(x)$ is the gamma function. When $0 < \beta \leq 1$, $b_\alpha > 1$. More interestingly, the ratio of the decay rates $B_\epsilon/B_\Omega = (b_\epsilon/b_\Omega)^\beta$ can be analytically obtained as

$$\frac{B_\epsilon}{B_\Omega} = \left(\frac{b_\epsilon}{b_\Omega}\right)^\beta = \left(\frac{\Gamma\left(\frac{N_\epsilon+2}{2\beta}\right)}{\Gamma\left(\frac{N_\epsilon}{2\beta}\right)} \frac{\Gamma\left(\frac{N_\Omega}{2\beta}\right)}{\Gamma\left(\frac{N_\Omega+2}{2\beta}\right)}\right)^\beta > 1. \tag{10}$$

For $N_\epsilon = 5$, $N_\Omega = 3$, and $0 < \beta \leq 1$ all arguments of the gamma functions in Eq. (10) are greater than $3/2$, for which $\Gamma(x)$ and $\ln\Gamma(x)$ are convex and monotonically increase as functions of x. Therefore, we have the inequality $B_\epsilon/B_\Omega = (b_\epsilon/b_\Omega)^\beta > 1$; thus for left and right tails and for any Reynolds number we have

$$P(\epsilon) < P(\Omega). \tag{11}$$

When R_λ is infinite, the β would be small, and we can compute the ratio using Stirling's formula for the gamma function to the leading order of small β as

$$\frac{B_\epsilon}{B_\Omega} \to e^{\frac{1}{2}[(N_\epsilon+2)\ln(N_\epsilon+2)-N_\epsilon \ln N_\epsilon]} \times e^{\frac{1}{2}[N_\Omega \ln N_\Omega-(N_\Omega+2)\ln(N_\Omega+2)]} \approx 1.51. \tag{12}$$

The ratio of the decay rates can be described solely by N_ϵ and N_Ω, and independent of β. Figure 2(b) indicates that B_ϵ/B_Ω obtained by the DNSs is greater than unity, decreases very slowly with R_λ, and tends to an asymptotic value which is about 10% smaller than 1.51 of Eq. (12). This is in agreement with the theoretical prediction [Eq. (10)] that is computed by using β of DNS, and also consistent with the data by Ref. [6]. The underestimation of the ratio by DNS is due to the fact that the peak part of Eq. (7) is smaller than the actual PDFs.

Equations (10)–(12) and DNS results in the previous arguments strongly suggest that the number of terms (degrees of freedom) contributing to the dissipation rate and enstrophy determines the power law exponents of the left tails and the decay rates B_α of the right tails of the PDFs [12], while the stretching exponent β is related to the singularities of the Navier-Stokes equation and their likeliness. Moreover they lead to the following predictions.

PDFs of the dissipation surrogates.—The dissipation surrogates $\tilde{\epsilon}_n$ $(n = 1, \ldots, 4)$ are defined by the sum of n terms as

$$\begin{aligned} \tilde{\epsilon}_1 &= 2\nu e_{11}^2, \qquad \tilde{\epsilon}_2 = 2\nu(e_{12}^2 + e_{23}^2), \\ \tilde{\epsilon}_3 &= 2\nu(e_{12}^2 + e_{13}^2 + e_{23}^2), \\ \tilde{\epsilon}_4 &= 2\nu[e_{11}^2 + 2(e_{12}^2 + e_{13}^2 + e_{23}^2)], \end{aligned} \tag{13}$$

where $e_{ij} = \frac{1}{2}(\partial u_i/\partial x_j + \partial u_j/\partial x_i)$ is the rate of strain tensor. The above theoretical arguments based on Eqs. (10)–(12) predict that (a) the left PDF tails are of the power laws with exponents $\sigma_n = n/2 - 1$, and (b) the stretching exponents are all the same but the decay rates increase with n, so that (c) $P(\epsilon) < P(\epsilon_4) < \cdots < P(\epsilon_1)$ for the left and right tails, regardless of R_λ. Indeed, the accuracy of these predictions can be clearly seen in Fig. 3. The right PDF tails expand with decreasing n in Fig. 3(a), and the slope of the left tails of the PDFs changes as $n/2 - 1$, so that $P(\epsilon_1)$ has a cusp for very small ϵ_1 in Fig. 3(b). On the other hand, in Fig. 3(c), the curves of the compensated PDFs for large amplitudes tend to be all parallel, and the stretching exponents of the right tails are the same as 0.21 regardless of n.

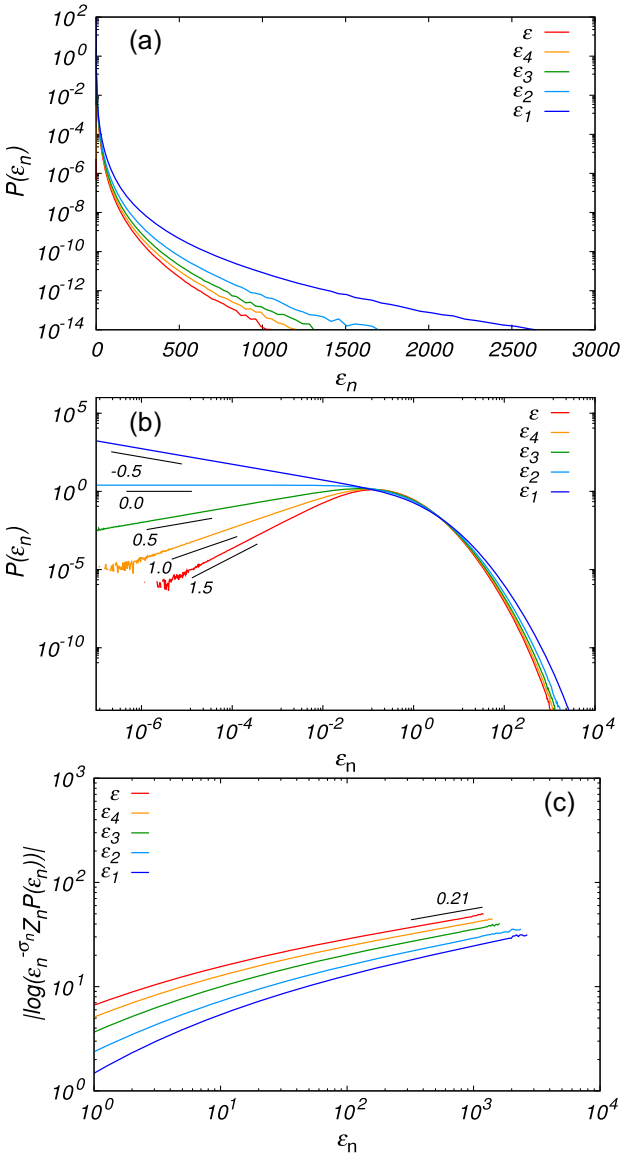

FIG. 3. PDFs of ϵ_n for Run 2048C, $R_\lambda = 358$. (a) logarithm-linear plot, (b) logarithm-logarithm plot, (c) compensated PDFs $|\ln[\epsilon^{-\sigma_n} Z_n P(\epsilon_n)]|$. Red, ϵ; orange, ϵ_4; green, ϵ_3; cyan, ϵ_2; blue, ϵ_1. Straight lines and numbers show the slopes of the curves.

An important suggestion of our findings is that the exponent β can be obtained by measuring the right tail of $P(\epsilon_1)$ in very high Reynolds number experiments, in which the measurement of ϵ_1 is much easier than that of ϵ.

Moments of the dissipation rate and enstrophy.—Although the expressions (7) and (9) are for asymptotic tails, the pth order moments are computed by substituting Eq. (7) into $\int_0^\infty x^p P_\alpha(x)dx$ as

$$\langle \epsilon^p \rangle = \left[\frac{\Gamma\left(\frac{5}{2\beta}\right)}{\Gamma\left(\frac{7}{2\beta}\right)}\right]^p \frac{\Gamma\left(\frac{5+2p}{2\beta}\right)}{\Gamma\left(\frac{5}{2\beta}\right)}, \tag{14}$$

$$\langle \Omega^p \rangle = \left[\frac{\Gamma\left(\frac{3}{2\beta}\right)}{\Gamma\left(\frac{5}{2\beta}\right)} \right]^p \frac{\Gamma\left(\frac{3+2p}{2\beta}\right)}{\Gamma\left(\frac{3}{2\beta}\right)}. \quad (15)$$

However, the moments with the order $p \leq -5/2$ for the dissipation rate and $p \leq -3/2$ for the enstrophy do not exist. For $p = 2$ and the Gaussian random field for which $\beta = 1$,we obtain $\langle \Omega^2 \rangle - \langle \epsilon^2 \rangle = 4/15 > 0$ as shown by Ref. [2].

Effects of spatial dimensions on PDFs.—Therefore, the more that terms are included in the sum of the dissipation (surrogate) and the enstrophy, the smaller the fluctuations and the shorter the PDF tails are, which is the same mechanism as for the central limit theorem. In this regard, it is worth considering the effect of the spatial dimension d. DNS of four-dimensional turbulence showed that the cumulative PDF $P_c(\epsilon) = \int_\epsilon^\infty P(\epsilon')d\epsilon'$ in $d = 4$ is considerably narrower than $P_c(\epsilon)$ in $d = 3$ [16]. This can be understood by considering the fact that $N_\epsilon(d)$ and $N_\Omega(d)$ are quadratic functions of d, and the power law exponents $N_\alpha(d)/2 - 1$ of the left tail and decay rates B_α of the right tail of Eq. (7) increase rapidly with d, while the stretching exponent β is expected to change slowly with d, because the increase in the number of terms leads to weak fluctuation of the amplitudes around the mean. It is conjectured that when $d > 3$, the left and right tails of PDF $P_{\alpha,d}(x)$ in d-dimensional space would satisfy $P_{\alpha,d\geq 4}(x) < P_{\alpha,d=3}(x)$ and $P_d(\epsilon) < P_d(\Omega)$ irrespective of R_λ.

With regard to the question asked in the introduction, *why does the enstrophy PDF have a longer tail than the dissipation PDF*, we conclude that although the straining motion and vorticity describe different aspects of fluid motion, the different tail behavior between two PDFs arises from the different number of terms contributing to the dissipation rate and enstrophy, which is the kinematic constraint. Elucidation of the physics and development of the mathematics needed for determination of β and its relation to the singularities of the Navier-Stokes equation, and their likeliness, are major challenges in turbulence research.

The authors deeply thank Dr. Buaria for his comments and kindness of providing the PDF data of the dissipation and enstrophy in Figs. 1 and 2. This work was supported by JSPS KAKENHI Grant No. JP20H00225 for T. G, JP20H02066 for I. S. and JP18K03925 for T. W. High Performance Computing Infrastructure (HPCI, hp220054), Networking, Large-Scale Data Analyzing and Information Systems (JHPCN, jh220003), and the National Institute for Fusion Science (NIFS22KISS002) are gratefully acknowledged for providing computational resources.

*gotoh.toshiyuki@nitech.ac.jp
†watanabe@nitech.ac.jp
‡saito.izumi@nitech.ac.jp

[1] S. Chen, K. R. Sreenivasan, and M. Nelkin, Inertial Range Scalings of Dissipation and Enstrophy in Isotropic Turbulence, Phys. Rev. Lett. **79**, 1253 (1997).
[2] H. Chen and S. Chen, Kinematic effects on local energy dissipation rate and local enstrophy in fluid turbulence, Phys. Fluids **10**, 312 (1998).
[3] B. W. Zeff, D. D. Lanterman, R. McAllister, R. Roy, E. J. Kostelich, and P. Lathrop, Measuring intense rotation and dissipation in turbulent flows, Nature (London) **421**, 146 (2003).
[4] D. A. Donzis, P. K. Yeung, and K. R. Sreenivasan, Dissipation and enstrophy in isotropic turbulence: Resolution effects and scaling in direct numerical simulations, Phys. Fluids **20**, 045108 (2008).
[5] P. K. Yeung, X. M. Zhai, and K. R. Sreenivasan, Extreme events in computational turbulence, Proc. Natl. Acad. Sci. U.S.A. **112**, 12633 (2015).
[6] P. K. Yeung, K. R. Sreenivasan, and S. B. Pope, Effects of finite spatial and temporal resolution in direct numerical simulations of incompressible isotropic turbulence, Phys. Rev. Fluids **3**, 064603 (2018).
[7] D. Buaria, A. Pumir, E. Bodenschatz, and P. K. Yeung, Extreme velocity gradients in turbulent flows, New J. Phys. **21**, 043004 (2019).
[8] D. Buaria, A. Pumir, and E. Bodenschatz, Self-attenuation of extreme events in Navier-Stokes turbulence, Nat. Commun. **11**, 5852 (2020).
[9] D. Buaria, A. Pumir, and E. Bodenschatz, Vortex stretching and enstrophy production in high Reynolds number turbulence, Phys. Rev. Fluids **5**, 104602 (2020).
[10] T. Gotoh and J. Yang, Transition of fluctuations from Gaussian state to turbulent state, Phil. Trans. R. Soc. A **380**, 20210097 (2021).
[11] D. Buaria and A. Pumir, Vorticity-Strain Rate Dynamics and the Smallest Scales of Turbulence, Phys. Rev. Lett. **128**, 094501 (2022).
[12] P. K. Yeung, D. A. Donzis, and K. R. Sreenivasan, Dissipation, enstrophy and pressure statistics in turbulence simulations at high Reynolds numbers, J. Fluid Mech. **700**, 5 (2012).
[13] See Supplemental Material at http://link.aps.org/supplemental/10.1103/PhysRevLett.130.254001 for the method and accuracy of DNS, the numerical parameters and data of the stretched exponents and decay rates.
[14] T. Gotoh, D. Fukayama, and T. Nakano, Velocity field statistics in homogeneous steady turbulence obtained using a high-resolution direct numerical simulation, Phys. Fluids **14**, 1065 (2002).
[15] J. Schumacher, K. R. Sreenivasan, and P. K. Yeung, Very fine structures in scalar mixing, J. Fluid Mech. **531**, 113 (2005).
[16] E. Suzuki, T. Nakano, N. Takahashi, and T. Gotoh, Energy transfer and intermittency in four-dimensional turbulence, Phys. Fluids **17**, 081702 (2005).